International Journal of
Geo-Information

Article

Exploring the Connection between Urban 3D Form and Building Energy Performance and the Influencing Mechanism

Deng Wang [1,2], Guoqin Zhang [1,3], Tao Lin [1,3], Xinyue Hu [1,3,4], Zhuoqun Zhao [1,2] and Longyu Shi [1,3,*]

1 Key Lab of Urban Environment and Health, Institute of Urban Environment, Chinese Academy of Sciences, Xiamen 361021, China; wangdeng@iue.ac.cn (D.W.); gqzhang@iue.ac.cn (G.Z.); tlin@iue.ac.cn (T.L.); xinyue.hu@stud.sbg.ac.at (X.H.); zqzhao@iue.ac.cn (Z.Z.)
2 University of Chinese Academy of Sciences, Beijing 100049, China
3 Xiamen Key Laboratory of Urban Metabolism, Xiamen 361021, China
4 Department of Geography and Geology, University of Salzburg, 5020 Salzburg, Austria
* Correspondence: lyshi@iue.ac.cn

Abstract: Continuous growth of building energy consumption CO_2 emission (BECCE) threatens urban sustainable development. Urban form is an important factor affecting BECCE. Compactness is a significant urban morphological characteristic. There is currently a lack of research on the effect of urban three-dimensional (3D) compactness on BECCE. To clarify the research value of 3D compactness, we investigated whether 3D compactness has a stronger impact on BECCE than two-dimensional (2D) compactness. A total of 288 buildings of the People's Bank of China (PBOC) were divided into 5 zones according to building climate demarcation. As BECCE is affected mainly by four aspects (socioeconomic condition, building features, macroclimate, and urban form), the BECCE driven by urban form (BECCE-f) in each zone was calculated firstly using the partial least square regression model. Normalized compactness index (NCI) and normalized vertical compactness index (NVCI) were calculated with Python to quantify urban 2D and 3D compactness within a 1 km buffer of PBOC buildings. The mean NCI and NVCI values of each zone were adopted as 2D and 3D compactness of this zone. Gray correlation analysis of the five zones showed that the connection between the NVCI and BECCE-f is stronger than that between NCI and BECCE-f. Based on this, we believe that the emphasis of later research should be shifted to urban 3D form, not just 2D elements. 3D form can describe the real urban form in a more accurate and detailed manner. Emphasizing 3D morphological characteristics in studies of the relationship between urban form and building energy performance is more meaningful and valuable than only considering 2D characteristics. The impact mechanism of urban form on BECCE-f should also be analyzed from the perspective of 3D form. This study also provides beneficial solutions to building energy saving and low-carbon building construction.

Keywords: 3D compactness; building microclimate environment; office building; energy consumption CO_2 emission; partial least square

check for updates

Citation: Wang, D.; Zhang, G.; Lin, T.; Hu, X.; Zhao, Z.; Shi, L. Exploring the Connection between Urban 3D Form and Building Energy Performance and the Influencing Mechanism. *ISPRS Int. J. Geo-Inf.* **2021**, *10*, 709. https://doi.org/10.3390/ijgi10100709

Academic Editor: Wolfgang Kainz

Received: 16 August 2021
Accepted: 10 October 2021
Published: 16 October 2021

1. Introduction

The building energy consumption CO_2 emission (BECCE) we studied is CO_2 emission from building operational energy consumption, which refers to energy utilization concerning building heating, cooling, lighting, and other activities [1]. From 2005 to 2018, the energy consumption of building operational activities and relevant CO_2 emission presented a trend of continuous growth [2]. In 2019, building operational energy consumption was responsible for about 22% of the total energy consumption in China, generating 2.2 billion tons of CO_2 emissions [3]. The building sector is the second-largestCO_2 emissions source in China [4]. Therefore, energy conservation and emission reduction of the building sector can make a significant contribution to China's performance in CO_2 mitigation commitments [5]. With the expansion of urban built-up areas, the continued growth of building stock, and the improvement of living standards, it is predicted that BECCE will increase continuously and become a constraint on urban sustainable development [6].

Regulations usually neglect the significance of urban form and geometry in designing urban sustainable development [7]. Urban form can affect urban microclimate environment, including thermal environment, ventilation, reflection, and absorption of solar radiation, etc. [8–13]. Research shows that the distribution of microclimate is subject to urban morphology [14]. Microclimate environment will further influence building energy consumption and CO_2 emission [12,15–17]. Compactness is an important urban morphological characteristic. The compact city is generally believed to be a necessary and sustainable urban development model, especially against this backdrop of population explosion and limited land resources [18,19]. In terms of energy use and carbon emissions in compact cities, because of the properties of travel distance and trip mode, research has mainly paid attention to the transportation sector [20–23]. In studies concerning the effect of urban form on building energy consumption and CO_2 emission, however, urban compact form is rarely considered [24].

Currently, research on the effect of urban form on building energy consumption mostly focuses on 2D urban form [25–28]. The planar layout and pattern, such as building density and land-use pattern, are the main research objects [24]. The real urban form includes not only the 2D pattern but also the 3D attribute, such as the spatial geometry and the intensity of space utilization in a 3D space. However, there is a lack of research on the effect of urban 3D form, let alone 3D compactness, on BECCE. A major reason is the acquisition of 3D morphological parameters, and the quantification of 3D urban form is difficult in empirical studies, which makes it so a lot of research can only be conducted under simulation scenarios and hypothetical conditions [29–31]. To conduct similar research, we should first examine whether there is a strong connection between urban 3D compactness and BECCE, and what is the impact mechanism of 3D compactness on BECCE in different climate zones.

BECCE is primarily affected by many factors, which can be summarized into four main aspects: socioeconomic condition, building features, macroclimate, and urban form [32,33]. Most studies use only the original total BECCE value to explore the relationship between BECCE and its influence factor. Under this condition, the result will inevitably be interfered with by other factors that we do not care about. Some studies have explored the regression method to eliminate the effects of household social and economic conditions on residential building energy consumption [28,34,35]. In our study, to calculate BECCE driven by urban form and improve research accuracy, the effects of nontarget factors (socioeconomic condition, building features, and macroclimate) on BECCE should be eliminated.

Typical office buildings (i.e., PBOC buildings) in China are taken as examples in this study. The main aims and highlights are: (1) eliminating the effects of nontarget factors on BECCE, calculating the BECCE-f, (2) investigating whether there is a stronger connection between 3D compactness and BECCE-f than that between 2D compactness and BECCE-f, and (3) exploring the influential mechanism of urban form on BECCE-f from the perspective of 3D compact form. It is considered that this research can provide a method and perspective for later studies on the relationship between urban form and building energy performance and CO_2 emission and also provide a beneficial solution to building energy saving and low-carbon building construction.

2. Methods

A flow chart summarizing the methods is illustrated in Figure 1. Detailed methods and processes are introduced in Sections 2.1–2.4.

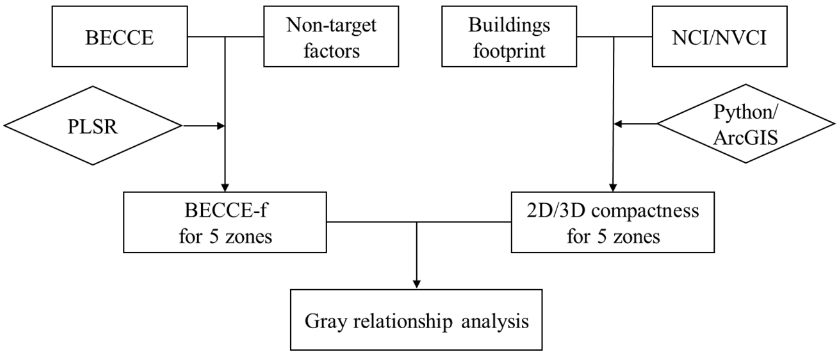

Figure 1. Flow chart of the basic methodology.

2.1. BECCE Calculation and Data Collection

Firstly, the BECCE of each PBOC building was calculated. The necessary data for future research, including building footprint and the condition of nontarget factors, were also collected.

2.1.1. BECCE Calculation

We calculated BECCE based on the consumption data of 4 kinds of energy: electricity (10^4 kW·h), raw coal (t), natural gas (10^4 m^3), and heating power (GJ) in 2014. Consumption of these energies is related to the activities of office buildings (such as heating, cooling, and lighting). These activities are influenced by the microclimate created by urban form. The following formula was used to calculate BECCE:

$$BECCE = \sum_{i}^{n} Con_i * F_i \tag{1}$$

where *BECCE* is the building energy consumption CO_2 emission (tCO_2), Con_i is the consumption of energy i (i = 1, 2, 3, 4), F_i is the CO_2 emission coefficient of energy i, and n is the number of types of consumed energy.

2.1.2. Socioeconomic Condition, Building Features, and Macroclimate Data

Based on the literature review [4,5,12,32,36–38], combined with general knowledge, the secondary indicators of three nontarget factors (socioeconomic condition, building features, and macroclimate) were determined. These secondary indicators can better reflect the condition of the corresponding factor.

Education expenditure (EE, 10^4 yuan) and per-capita wage (PW, yuan) in the city municipal districts were selected as indicators of socioeconomic condition. China City Statistical Yearbook 2014 provided us with these data.

Building floor area (FA, m^2) and the number of energy users (EUs, person) were chosen as indicators representing building features. The PBOC buildings dataset contained this information.

Cooling degree day (CDD, °C d) based on 26 °C and heating degree day (HDD, °C d) based on 18 °C are quantitative indices reflecting the demand of building cooling and heating. CDD and HDD were used to represent the macroclimate condition in this study. CDD and HDD were calculated according to Formulas (2) and (3):

$$CDD = \sum_{i=1}^{365} (t_i - 26) * D \tag{2}$$

$$HDD = \sum_{i=1}^{365} (18 - t_i) * D \tag{3}$$

where t_i is the average daily outdoor temperature for i day, D = 1 d. When $(t_i - 26)$ or $(18 - t_i)$ is negative, take $(t_i - 26)$ and $(18 - t_i) = 0$.

We obtained the daily mean temperature data of 398 Chinese meteorology stations throughout 2014 from the Global Surface Summary of the Day (https://data.noaa.gov/dataset/dataset/global-surface-summary-of-the-day-gsod, accessed on: 5 January 2020) and calculated their CDD and HDD. A total of 288 PBOC buildings acquired their CDD and HDD value by interpolation, as shown in Figure 2.

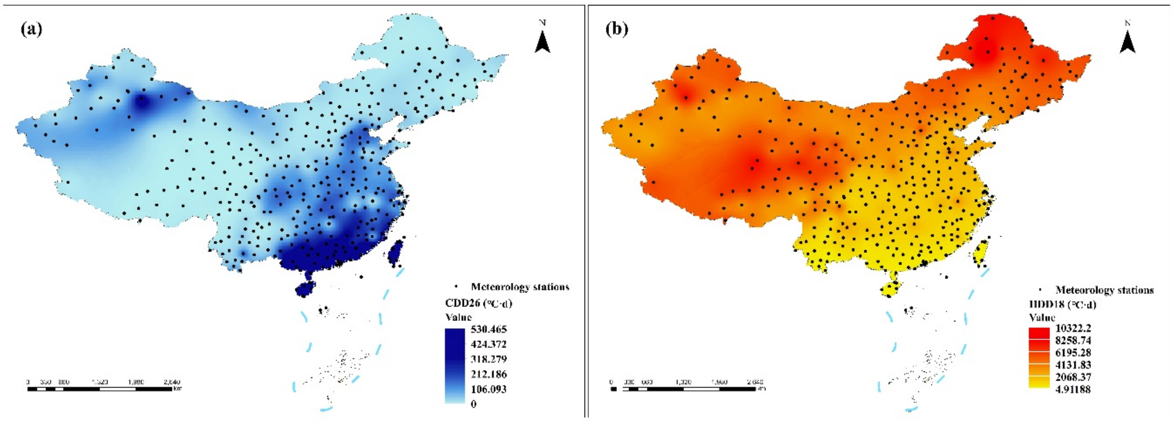

Figure 2. Distribution of CDD (**a**) and HDD (**b**). The darker the color, the higher the demand for cooling or heating.

2.1.3. Buildings Footprint Data

The influence of urban form on building energy performance and CO_2 emission is indirect. As mentioned above, urban form influences BECCE by affecting the building microclimate environment. Hence, research of the effect of urban form on BECCE should be conducted from the perspective of building microclimate, which refers to the local climate within a radius of 1 km around the building, as shown in Figure 3a [39]. 2D and 3D compactness within a 1 km buffer area of individual buildings was selected as an indicator of urban form. Building footprint data we collected contained the building area and height information. Example data in the 2D pattern are shown in Figure 3b, and its corresponding 3D form is shown in Figure 3c.

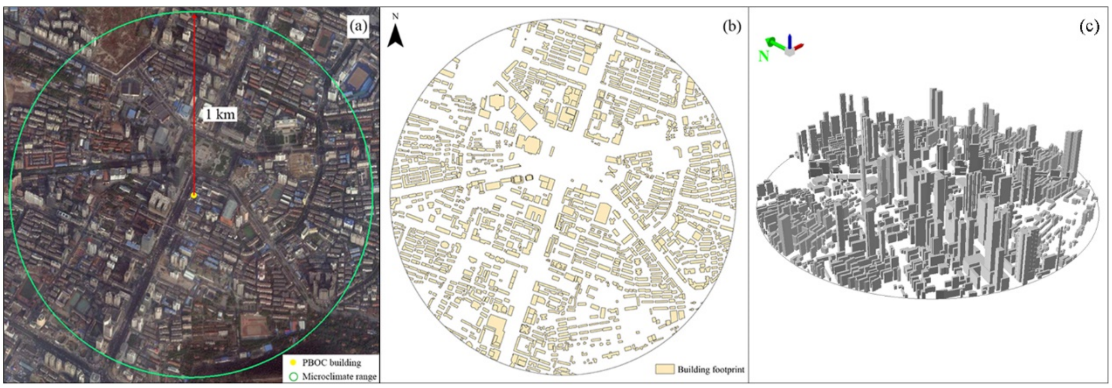

Figure 3. Diagram of the 1 km buffer for a PBOC building (**a**), 2D pattern of the buildings in the buffer area (**b**), and 3D form (displayed after stretching) of the buildings in the buffer area (**c**).

2.2. Calculating BECCE-f

Next, the BECCE and nontarget factors were used to eliminate the effects of nontarget factors on BECCE and calculate BECCE-f by the specific method in this study.

2.2.1. Basic Principle

The 288 PBOC buildings were divided into 5 zones according to the building climate demarcation depicted in Figure 4: hot summer/warm winter zone (HSWW), hot summer/cold winter zone (HSCW), mild zone (ML), cold zone (CL), and severe cold zone (SC).

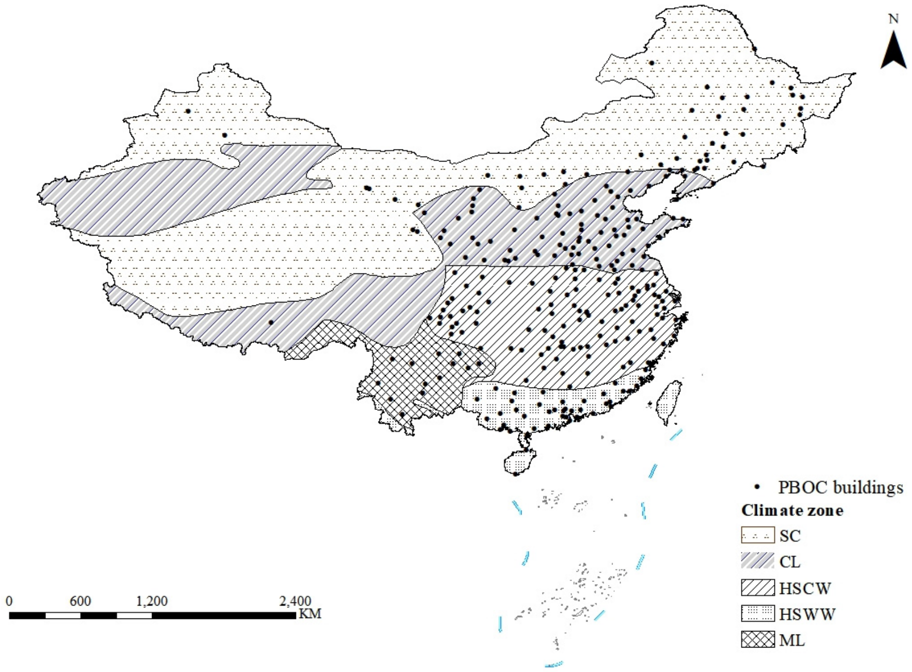

Figure 4. China's building climate demarcation and the distribution of 288 PBOC buildings.

To obtain the BECCE-f of each zone, the nontarget factors' interference should be eliminated, including socioeconomic condition, building features, and macroclimate. That means the three factors of the 5 zones should be kept consistent with each other. In each zone, taking BECCE as the dependent variable and *EE*, *PW*, *FA*, *EU*, *CDD*, and *HDD* as independent variables, we first set up the regression model between them. When keeping the other three factors as the average level—a standardized unit—the BECCE of this standardized unit should be the same in every zone because the three driving factors are the same. The fact is there are differences between the zones when this standardized unit is put into a different zone. These differences were believed to be driven by the fourth driving factor, i.e., the target factor—urban form. Hence, the respective mean value of *EE*, *PW*, *FA*, *EU*, *CDD*, and *HDD* of all 288 buildings was then put into 5 regression models to calculate BECCE driven by the urban form of each zone.

Considering the collinearity of independent variables, the partial least square regression (PLSR) method was chosen to calculate BECCE-f.

2.2.2. PLSR

The partial least square method combines the advantages of both principal component analysis and canonical correlation analysis. It is applicable to the data characterized by collinearity. The basic theory can be summarized as follows [40,41].

Assuming there are independent variables matrix $X = [x_1, x_2, \ldots, x_m]$ and dependent variable y. X can be decomposed as Formula (4):

$$X = TP^T + E \tag{4}$$

where T is a latent factor matrix, P is a loading vector matrix, and E is the residual matrix of X. The basis for the PLSR is that the relation between X and y can be conveyed by the latent factors. This means that y can also be decomposed as:

$$y = Tq^T + f \tag{5}$$

where q is the loading value of y, and f is the residual vector of y. Predicted dependent variable $\hat{y}$ is computed through the following linear equation:

$$\hat{y} = Xb \tag{6}$$

where b is an array of regression coefficients.

In our study, PLSR models were established in R software and tested with the method of leave-one-out cross-validation.

2.3. 2D and 3D Compactness

The compactness index (CI) is based on Newton's law of gravitation [42]. It quantifies the urban 2D compactness by gridding the construction land and calculating the average gravitation of the spatial interaction of urban land use. CI is significantly affected by the scale of an urban built-up area. To offset this shortcoming, the normalized compactness index (NCI) was developed [43]. It assumes that a round city has the greatest compactness because the urban space is fully occupied by construction land. NCI is defined as the ratio of the actual urban construction land to its equivalent circular land, whose area is equal to the target city's construction area. The compactness of equivalent circular land is used as a normalized factor in the NCI to normalize CI between 0 and 1, which makes it convenient to compare the urban 2D compactness among different cities. The NCI is given by:

$$\mathrm{NCI} = \frac{\mathrm{CI}}{\mathrm{CI_{round}}} = \frac{\mathrm{M(M-1)}}{\mathrm{N(N-1)}} * \frac{\sum_{\mathrm{i}}^{\mathrm{n}} \sum_{\mathrm{i}}^{\mathrm{n}} \frac{\mathrm{Z_i Z_j}}{\mathrm{d^2(i,j)}}}{\sum_{\mathrm{i'}}^{\mathrm{n}} \sum_{\mathrm{j'}}^{\mathrm{n}} \frac{\mathrm{S_i' S_j'}}{\mathrm{d'^2(i',j')}}} \tag{7}$$

where CI is the average gravity of urban spatial interaction, (i.e., the compactness of urban spatial form), $\mathrm{CI_{round}}$ is the compactness of the round city, N is the total number of grids of construction land, M is the total number of grids of the round city, $\mathrm{Z_i}$ and $\mathrm{Z_j}$ represent the urban construction land area ($\mathrm{i} \neq \mathrm{j}$) in any two grids i and j, d (i, j) is the geometric distance between grid i and grid j, and $\mathrm{S_i}'$ and $\mathrm{S_j}'$ are construction land areas of grids i ' and j ' in the round city.

The normalized vertical compactness index (NVCI) indicates the compactness of urban 3D spatial form by the strength of the spatial gravitation between urban buildings [44,45]. A sphere is the most compact 3D spatial form in the universe because of gravity. The equivalent sphere of a city refers to the sphere whose volume is equal to the urban buildings' volume. NVCI is defined as the ratio of actual 3D urban spatial form to its equivalent sphere. The equivalent sphere was taken as the normalized factor in the NVCI to eliminate errors caused by city scale differences. The NVCI calculation formula is:

$$\mathrm{NVCI} = \frac{\mathrm{VCI}}{\mathrm{VCI_{max}}} = \frac{\mathrm{P(P-1)}}{\mathrm{Q(Q-1)}} * \frac{\sum_{\mathrm{i}}^{\mathrm{n}} \sum_{\mathrm{i}}^{\mathrm{n}} \frac{\mathrm{V_i V_j}}{\mathrm{d^2(i,j)}}}{\sum_{\mathrm{i'}}^{\mathrm{n}} \sum_{\mathrm{j'}}^{\mathrm{n}} \frac{\mathrm{V_i' V_j'}}{\mathrm{d'^2(i',j')}}} \tag{8}$$

where VCI is vertical compactness index, $\mathrm{VCI_{max}}$ is the compactness of the equivalent sphere, P is the total number of cubes that the equivalent sphere occupies, Q is the number of all cubes, $\mathrm{V_i}$ and $\mathrm{V_j}$ are the volume of urban buildings in urban cube i and cube j ($\mathrm{i} \neq \mathrm{j}$), d(i, j) is the geometric distance between centroids of urban cube i and j, and $\mathrm{V'_i}$ and $\mathrm{V'_j}$ are the volumes of the equivalent sphere in the cube i′ and j′ (Figure 5). The value of NVCI is between 0 and 1, and the spatial form is more compact as the value approximates 1.

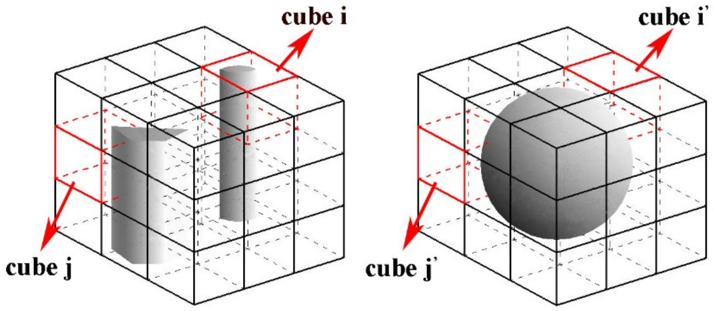

Figure 5. Schematic diagram of the spatial grid division of the NVCI. The left picture is the spatial grid division for the buildings, and the right picture is for the equivalent sphere.

For batch processing and convenient computation, two programs calculating the NCI and NVCI, respectively, were developed with Python and ArcGIS.

2.4. Gray Relationship Analysis

Gray relationship analysis is based on the geometric corresponding relationship between factors, and gray correlation degree (GCD) can describe the strength and extent of the connection between factors [46].

Assuming there is a reference sequence $X_0 = \{x_0(k), k = 1, 2, \ldots, n\}$, and a factor sequence $X_i = \{x_i(k), k = 1, 2, \ldots, n\}$, $(i = 1, 2, \ldots, m)$. The GCD between X_0 and X_i is defined as:

$$\gamma(X_0, X_i) = \frac{1}{n}\sum_{k=1}^{n}\gamma(x_0(k), x_i(k)), \quad (9)$$

$$\gamma(x_0(k), x_i(k)) = \frac{\mathrm{Min}_i\mathrm{Min}_k|x_0(k) - x_i(k)| + \rho\mathrm{Max}_i\mathrm{Max}_k|x_0(k) - x_i(k)|}{|x_0(k) - x_i(k)| + \rho\mathrm{Max}_i\mathrm{Max}_k|x_0(k) - x_i(k)|} \quad (10)$$

where ρ is the distinguishing coefficient, and $\rho \in [0, 1]$, normally $\rho = 0.5$. The matrix of GCD can be obtained by sorting the GCD in descending order. Then, the strength of the connection between X_0 and factors X_i can be judged.

Gray relationship analysis is applicable for the data with a small number of representative samples. Taking the BECCE-f as a reference sequence and the NCI and NVCI as factor sequences, we calculated GCD in a data processing system (DPS) to investigate the connections between urban 2D and 3D compactness and BECCE-f among the 5 zones.

3. Results and Discussion

3.1. BECCE of PBOC Buildings

As depicted in Figure 6, high BECCE bars were primarily concentrated in the north and east of China, while low bars mainly appeared in south and west China. The result implies that, on the whole, the buildings in north and east China consume more energy and generate more CO_2 than the buildings in south and west China. This trend is similar to the conclusion of previous research [47–49]. CO_2 released from electricity consumption is dominant in most buildings' BECCE structure, especially in south China. Electricity is the main energy used in their daily activities, while in the north, CO_2 generated from heating power and raw coal consumption accounts for a considerable proportion. Because heating power and raw coal are important heating energy sources in the cold and severe cold zones, building heat load plays a dominant role, and the heating period is long [50].

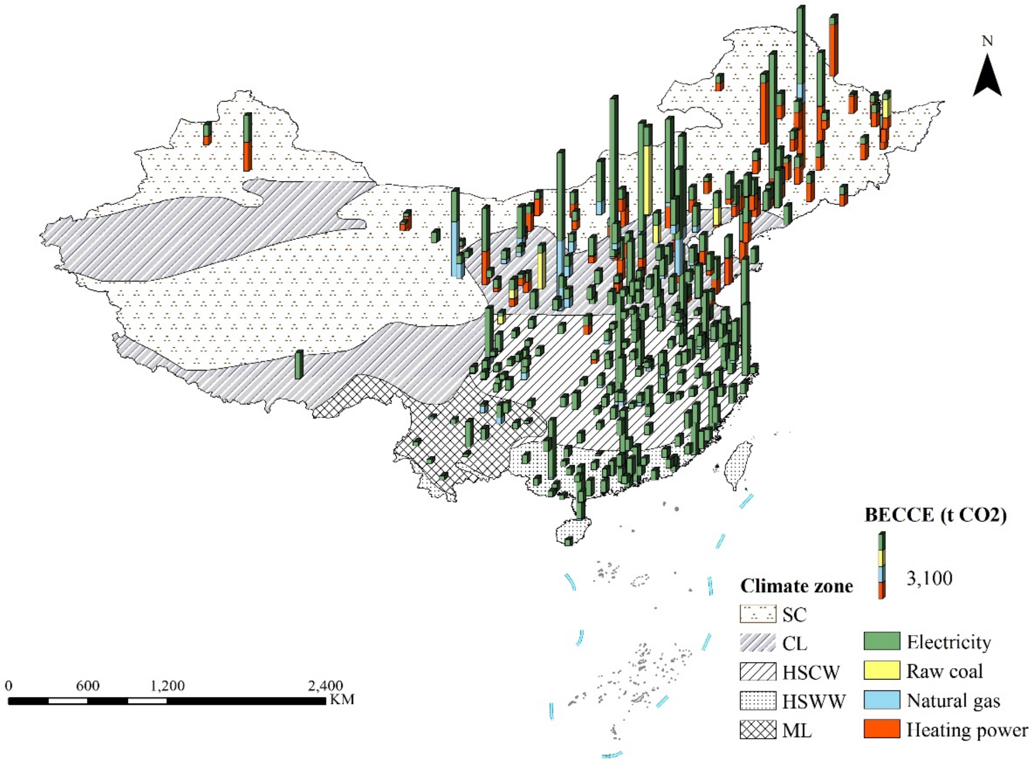

Figure 6. BECCE stacking diagram of 288 PBOC buildings. The higher histogram means a greater amount of BECCE. Histograms with different colors represent the BECCE generated by corresponding energy.

3.2. Description of Nontarget Factors

Figure 7 displays the minimum, mean, and maximum values of independent variables in each zone. For education expenditure, there are three extremely high values in CL, HSCW, and HSWW. They are 7,184,218, 6,773,006, and 3,308,000 (10^4 yuan), which, respectively, belong to Beijing, Shanghai, and Shenzhen, three megacities of China. It can be seen that the mean values of education expenditure of CL, HSCW, and HSWW are also relatively higher than the other two zones. The three regions spent more on education. There are few differences between mean values of the per-capita wage of the five zones. The highest per-capita wage appeared in HSCW (Tongren, 116,925.52 yuan), and the lowest exists in SC (Yichun, 24,631.43 yuan). ML has the least gap of per-capita wage between the maximum and minimum.

The differences in floor area and energy user among zones show the same trend, regardless of maximum, minimum, and mean values. PBOC buildings in ML have a relatively smaller floor area and fewer employees. PBOC buildings in regions with a high level of economic development usually have a larger floor area and more employees.

The macroclimate factors show a certain regularity among different zones. The SC has the lowest cooling degree day (i.e., the lowest cooling load), while the HSWW has the highest cooling degree day. On the contrary, HSWW has the lowest heating degree day (i.e., the lowest heating load), while SC has the highest heating degree day. There is a certain cooling load in CL and a certain heating load in HSCW. This regularity is associated with the location and the altitude. For example, ML is a low-latitude area, but its high altitude results in a lower cooling degree day and higher heating degree day.

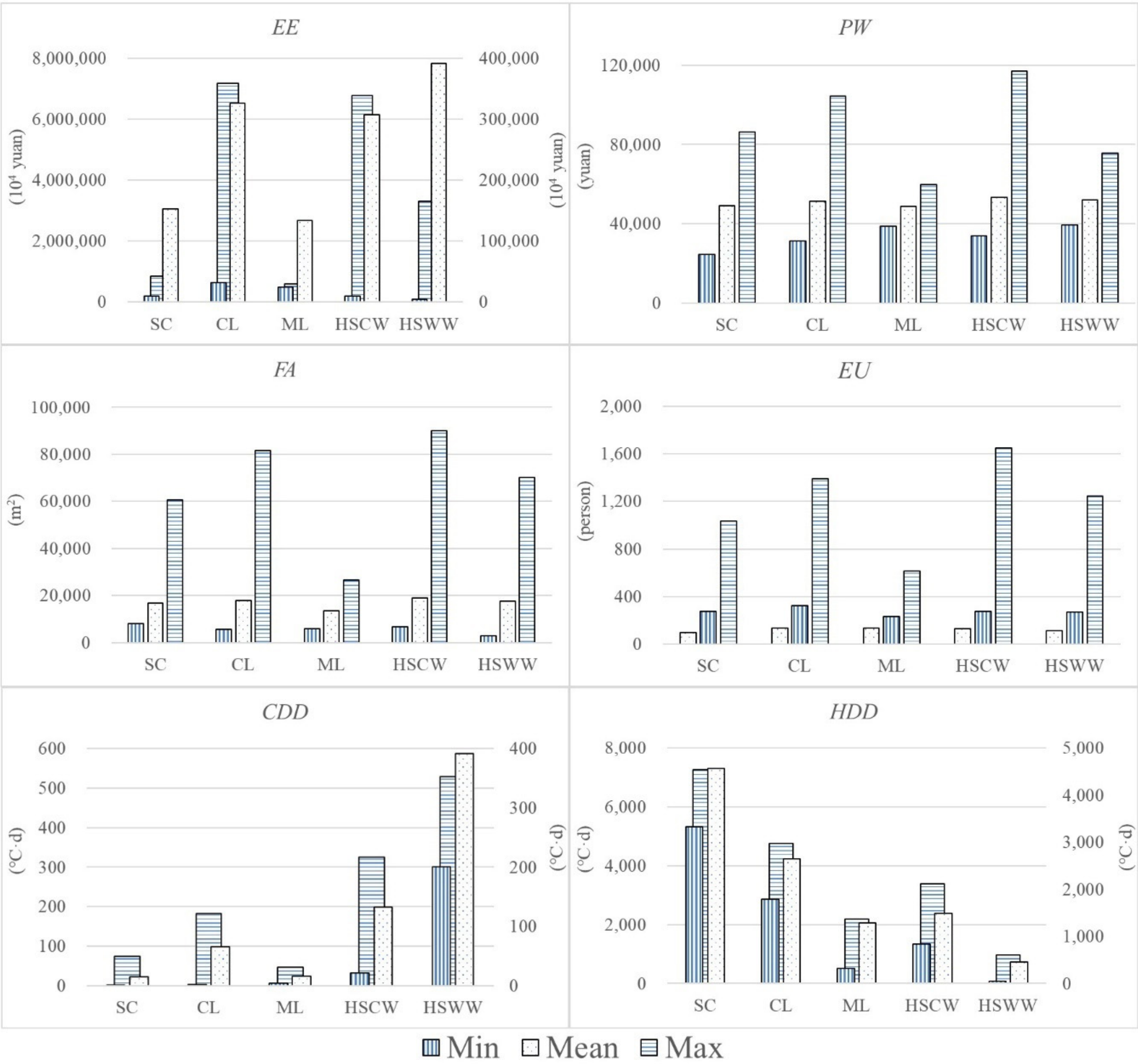

Figure 7. Minimum, mean, and maximum values of independent variables in each zone. Among them, the minimum and mean values of EE, CDD, and HDD are shown through the secondary ordinate axis on the right.

3.3. PLSR Models and BECCE-f

PLSR models are listed in Table 1. For each zone, *FA* and *EU* have a positive effect on BECCE, and the coefficients are relatively stable. The larger the floor area and the more energy consumed, the greater the BECCE. The higher *HDD* means a higher heating load, which can result in more BECCE in SC and CL. In HSWW, more cooling load can promote BECCE; thus, *CDD* has a positive correlation with BECCE. A cooler environment with higher *HDD* can reduce cooling energy consumption in HSWW. In HSCW, although the cooling load accounts for a large proportion of building air conditioning load, the heating load in winter also cannot be ignored. Therefore, both *CDD* and *HDD* have a positive effect on BECCE in HSCW. However, the negative effect of *CDD* and the positive effect of *HDD* on BECCE in ML might be due to the higher altitude. The higher the income, the greater the climate sensitivity of the energy consumed, which can cause more building energy consumption [51]. Strangely, the income has a negative effect on BECCE in SC, which needs further discussion. Income is often positively associated with education level, so the education level expressed by *EE* also has a positive effect on BECCE [52,53].

Table 1. PLSR models of the 5 zones.

Zones	PLSR Model	Adjusted-R^2
SC	$BECCE = -0.44 + 0.12EE - 0.47PW + 0.58FA + 0.40EU - 0.02CDD + 0.41HDD$	0.59
CL	$BECCE = -13.18 + 0.11EE + 0.70PW + 0.47FA + 0.46EU - 0.10CDD + 0.56HDD$	0.64
ML	$BECCE = -9.01 + 0.07EE + 0.66PW + 0.47FA + 0.19EU - 0.13CDD + 0.20HDD$	0.40
HSCW	$BECCE = -15.31 + 0.05EE + 0.78PW + 0.44FA + 0.54EU + 0.18CDD + 0.61HDD$	0.73
HSWW	$BECCE = -15.15 + 0.12EE + 1.25PW + 0.34FA + 0.50EU + 0.08CDD - 0.04HDD$	0.77

The mean values of *EE, PW, FA, EU, CDD*, and *HDD* of 288 samples were: 291,695.95 (10^4 yuan), 51,656.32 (yuan), 17,797.95 (m^2), 285 (person), 125.62 (°C d), and 2168.03 (°C d), respectively. Based on these mean values, the BECCE-f of each zone was calculated, as shown in Table 2.

Table 2. BECCE-f (tCO_2) of the 5 zones.

Zones	SC	CL	ML	HSCW	HSWW
BECCE-f (tCO_2)	765.1485	670.2507	240.5659	504.9595	355.4024

3.4. Urban 2D and 3D Compactness

Using Python programs, we calculated the NCI and NVCI values for each PBOC building.

3.4.1. Compactness Characteristics

For an intuitive comparison, Figure 8 depicts urban form in a 1 km buffer with the highest and lowest NCI and NVCI values.

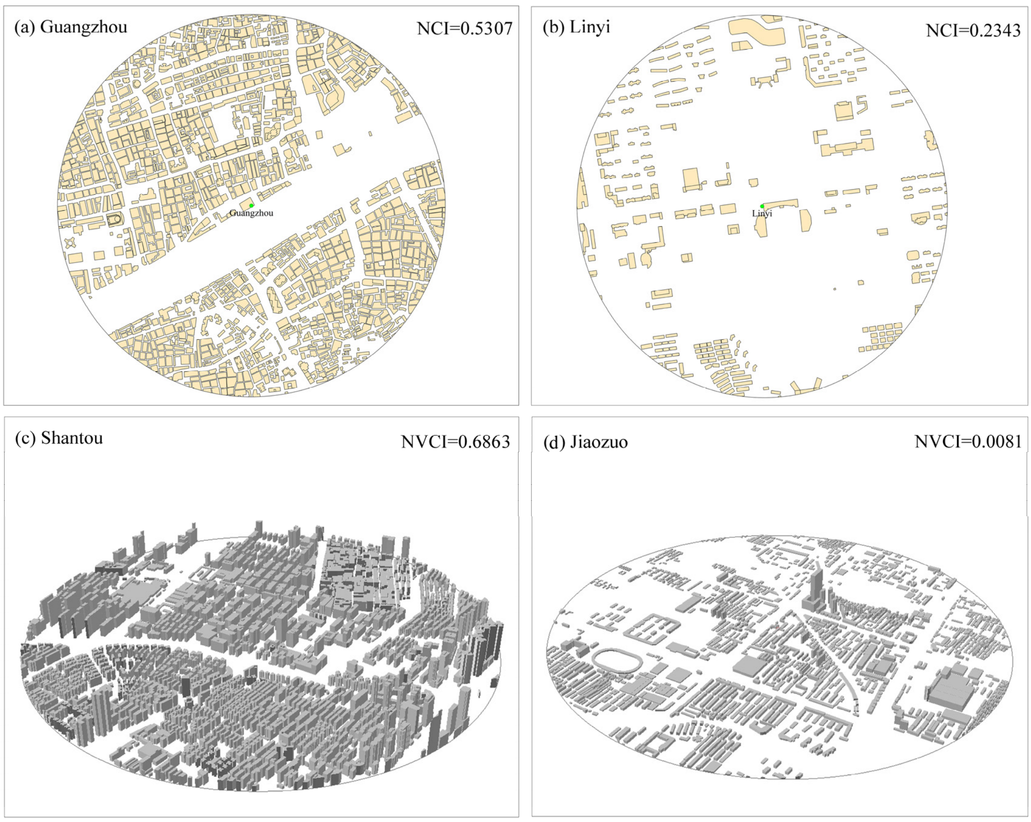

Figure 8. Urban form in a 1 km buffer with the maximum NCI (**a**), minimum NCI (**b**), maximum NVCI (**c**), and minimum NVCI (**d**). Urban form is more compact as NCI or NVCI approach 1.

As depicted in Figure 8a,b, the higher the NCI is, the denser the distribution of the buildings, and the more compact the urban form on a two-dimensional space, while a less compact form presents a relatively sparser distribution of the buildings. According to the principle of the NCI, a less 2D compact form signifies the interaction strength and connection among buildings is weaker [54]. The reasons for the formation of different urban compact forms are complex, including topography, hydrology, and social and economic conditions [54,55]. For example, as shown in Figure 8a, the strip-shaped blank area in the buffer of the Guangzhou PBOC building is the river. Without this river, it is estimated that the NCI will be higher.

It has been proven by a previous case study that the NVCI is positively correlated with building height and building density [44]. Similarly, in our study, the correlation coefficient between the NVCI and average buildings height is 0.35, and the correlation coefficient between the NVCI and buildings density is 0.45. However, the correlation coefficient between the NVCI and plot ratio (combining buildings density and average buildings height) reaches 0.63. Correspondingly, as shown in Figure 8c,d, buildings with a greater NVCI are denser and taller, and the urban form is more compact in a 3D space. The buildings with a lower NVCI showed a fewer, sparser, and lower pattern on the whole.

3.4.2. NCI and NVCI of the 5 Zones

Figure 9 shows the ranking of the NCI and NVCI of the five zones. The ML zone has the maximum NCI but the minimum NVCI. This means that the 2D form is the most compact in the ML zone, the layout of the buildings surrounding the PBOC building is denser. However, when the vertical attribute of buildings is taken into account, its form is the least compact. Urban form with the highest NCI does not necessarily has the highest NVCI because the vertical characteristics, such as building height and plot ratios of building, are different from each other.

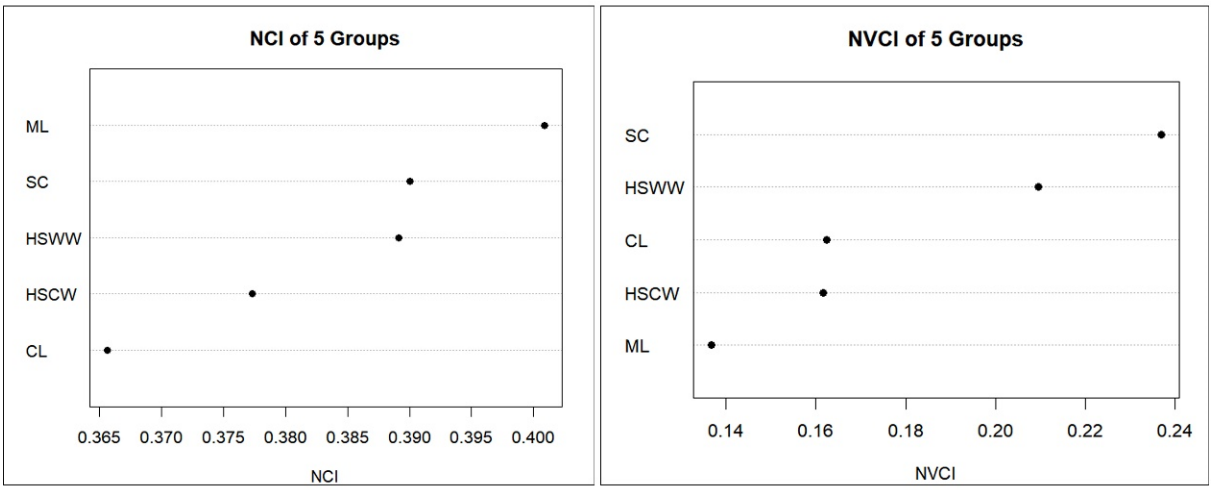

Figure 9. Ranking of mean NCI and NVCI values of the 5 zones.

3.5. Connection between BECCE-f and Urban Compactness

The NCI, NVCI, and BECCE-f of the five zones are listed in Table 3. Based on Table 3, we can calculate that the GCD between the BECCE-f and NCI is 0.51, and the GCD between the BECCE-f and NVCI is 0.69. This shows that the connection between the NVCI and BECCE-f was relatively stronger than the connection between NCI and BECCE-f. The results imply that, after the other factors' effects were eliminated, the NVCI had a more notable impact on BECCE-f. Compared to the NCI, the NVCI is a more applicable and more comprehensive index reflecting the effect of urban form on BECCE.

Table 3. The BECCE-f and NCI, NVCI of the 5 zones.

Zone	NCI	NVCI	BECCE-f
SC	0.3900	0.2370	765.1485
CL	0.3656	0.1624	670.2507
ML	0.4009	0.1367	240.5659
HSCW	0.3773	0.1616	504.9595
HSWW	0.3891	0.2096	355.4024

More comprehensive morphological information was taken into account in urban 3D form. Thus, 3D compactness is closer to the actual morphological characteristics of cities and can describe the real urban compact form in a more accurate and detailed manner than 2D compactness [44]. The impact mechanism of urban form through microclimate on BECCE can be reflected more comprehensively by urban 3D form than by 2D form. Therefore, the NVCI has a closer connection with BECCE-f than NCI. It can be inferred that emphasizing the 3D morphological characteristics in the study of the relationship between urban form and BECCE is more meaningful than considering 2D characteristics only.

4. Impact Mechanism of 3D Compactness on BECCE-f

As mentioned above, urban form can affect BECCE by influencing the urban microclimate environment, such as urban thermal environment, ventilation, reflection and absorption of solar radiation, etc. The study demonstrated that there is a positive relationship between land surface temperature and building density and building expandability, which refers to the utilization intensity of buildings to the space over the city [56]. The urban heat island (UHI) will be intensified in the area with high 3D compactness, where the larger building bodies absorb more solar shortwave radiation and store more heat. Moreover, the radiation is reflected multiple times among taller building façades that are closer to each other. The taller the buildings are, and the less uniform the building height is, the lower the albedo is [57]. Therefore, more solar radiation is captured at the top of the deep urban canyon. This abnormal absorption can lead to an increase in temperature inside the canyon [58]. The heat gain of buildings facades is thus increased, and the longwave radiation leaving the urban canopy is decreased [59,60].

In addition, the ventilation can also be affected by urban form. As tall and dense buildings result in less sky visible from the ground, higher 3D compactness will obviously cause a lower sky view factor (SVF). Lower site coverage and higher SVF can lead to a building's effective energy performance by enhancing urban ventilation [61,62]. Nevertheless, high-rise and high-density buildings will reduce the air ventilation channel and the speed of turbulent heat transport, resulting in hot air trapped between buildings [59,63]. Consequently, a kind of microclimate with a relatively higher temperature is created in the urban canyon. In hot regions where the cooling load dominates, such as HSWW and HSCW in this study, the cooling energy demand will increase considerably. In HSCW, the relatively higher temperature had a certain influence on their heating energy demand reduction in winter. In SC and CL, this microclimate will cause the reduction of heating energy consumption, especially in winter. Considering that the cooling demand is not strong in SC in summer, this microclimate has limited influence on building cooling in SC. However, the cooling demand in CL might increase. In ML, where the climate is moderate, the influence of urban form on BECCE is not very strong.

Dense high-rise buildings can shade the urban land surface and other buildings, creating more shadows in urban space. The shaded area usually has a lower temperature than the area directly shined on by the sun. Mutual shading can make a cooler microclimate environment. This is conducive to the reduction in building cooling energy consumption, especially in HSWW and HSCW in summer, but is adverse to the heating energy saving, especially in CL and SC in winter, where the solar gains are particularly limited and heating load plays a dominant role [64]. However, research has shown that mutual shading can cause the heating energy demand to increase even greater than the decrease in the cooling energy demand [65].

Increasing the area of urban green space and water body (GS&WB) and dispersing them are conducive to building energy saving [28,66]. However, GS&WB are facing space competition in compact cities, resulting in the loss of GS&WB area and the centralization of GS&WB [67]. This competition weakens the GS&WB ability of microclimatic regulation and energy saving advancement in compact cities.

Furthermore, there will be less sunlight accessibility in the area of high coverage of tall buildings, which can bring about more lighting requirements in buildings at afternoon or nightfall, particularly in cities at high latitude where light is scarce [64,68].

5. Conclusions

This study applied a regression method to eliminate the nontarget factors' effects on BECCE and calculated BECCE driven by urban form. Then, the NCI and NVCI of each zone were calculated. Finally, we explored the connection between urban 3D compactness and BECCE-f. Results of gray correlation analysis demonstrated that 3D compactness had a stronger connection with BECCE-f than 2D compactness. The analysis of the impact mechanism of 3D compactness on BECCE-f implied that urban 3D form surrounding an individual building significantly affects the overall building energy performance. This is the result of the influence of urban 3D compact form on building microclimate environment, including ventilation, thermal environment, and radiation environment.

Our studies proved that 3D form deserves more attention in research on the relationship between urban form and building energy consumption and CO_2 emission [69,70]. Urban 3D form takes into account more comprehensive morphological information. 3D form can describe the real urban compact form in a more accurate and detailed manner than 2D compactness. When investigating the impact mechanism of urban form on BECCE, considering 3D elements can definitely reflect the influencing mechanism more comprehensively than only considering 2D elements. It can be inferred that emphasizing the 3D morphological characteristics in the study of the relationship of urban form and building energy performance is more meaningful and valuable than considering 2D characteristics only. Currently, more eyes are being cast on 2D form (such as buildings floor area, building density, 2D layout and pattern, etc.), and research on the effect of urban 3D form on BECCE is still lacking. We believe that the emphasis of later research should be shifted to urban 3D form, not just 2D elements.

As we analyzed the influencing mechanism of 3D compact form on BECCE-f from the perspective of building microclimates, we believe this research can also provide guidance for city planners and building designers for the construction of low-carbon buildings and cities. Some directional measures promoting building energy conservation and emission reduction can be proposed accordingly. For instance, large and dispersed GS&WB was proven to be a feasible way of UHI mitigation [71]. Because of the limited land resources, GS&WB should integrate into compact cities in a new way. Roof greening and wall greening are practicable modes [72,73]. As for the building itself, the insulation performance of the exterior walls should be improved for a relatively constant indoor temperature and comfort. Albedo is a significant explanatory factor of urban land surface temperature [74]. The high reflection coating, which can reduce the heat gain of buildings, should be an increasing concern in the field of building materials and energy saving.

This study was based on building zoning, and one of the limitations is that we just calculated the BECCE-f of each zone. Future work should calculate the BECCE-f of each building using other methods, such as the downscaling method. Then, we simply demonstrated that the 3D compactness had a stronger connection with BECCE-f than 2D compactness. However, considering that the effect of urban 3D compactness on building energy performance displays a complicated pattern on a large scale, the potential linear or nonlinear relationship between urban 3D compact form and BECCE-f needs further exploration. Furthermore, a moderately compact form can be consequently discussed.

Author Contributions: Conceptualization, Deng Wang; methodology, Deng Wang, Guoqin Zhang, Xinyue Hu; software, Guoqin Zhang; validation, Deng Wang; formal analysis, Deng Wang; investigation, Deng Wang, Zhuoqun Zhao; resources, Longyu Shi; data curation, Deng Wang; writing—original draft preparation, Deng Wang; writing—review and editing, Deng Wang; visualization, Deng Wang, Xinyue Hu; supervision, Guoqin Zhang, Tao Lin; project administration, Tao Lin, Longyu Shi; funding acquisition, Tao Lin, Longyu Shi. All authors have read and agreed to the published version of the manuscript.

Funding: This research was funded by National Natural Science Foundation of China, Grant Number 71874174.

Institutional Review Board Statement: Not applicable.

Informed Consent Statement: Not applicable.

Data Availability Statement: Not applicable.

Acknowledgments: The authors would like to thank the editor, associate editor, and anonymous reviewers for processing our manuscript.

Conflicts of Interest: On behalf of all authors, the authors declare no conflict of interest.

Nomenclature

BECCE	building energy consumption CO_2 emission
3D	three-dimensional
2D	two-dimensional
BECCE-f	BECCE driven by urban form
PBOC	People's Bank of China
NCI	normalized compactness index
NVCI	normalized vertical compactness index
EE	education expenditure
PW	per-capita wage
FA	floor area
EU	energy users
CDD	cooling degree day
HDD	heating degree day
HSWW	hot summer/warm winter zone
HSCW	hot summer/cold winter zone
ML	mild zone
CL	cold zone
SC	severe cold zone
PLSR	Partial least square regression
GCD	gray correlation degree

References

1. Ye, H.; Wang, K.; Zhao, X.; Chen, F.; Li, X.; Pan, L. Relationship between construction characteristics and carbon emissions from urban household operational energy usage. *Energy Build.* **2011**, *43*, 147–152. [CrossRef]
2. China Association of Building Energy Efficiency. *Research Report on Building Energy Consumption in China*; China Association of Building Energy Efficiency: Xiamen, China, 2020.
3. Tsinghua University. *Annual Report on Chinese Building Energy Efficiency*; China Architecture & Building Press: Beijing, China, 2020.
4. Ye, H.; Ren, Q.; Hu, X.; Lin, T.; Xu, L.; Xu, L.; Li, X.; Zhang, G.; Shi, L.; Pan, B. Low-carbon behavior approaches for reducing direct carbon emissions: Household energy use in a coastal city. *J. Clean. Prod.* **2017**, *141*, 128–136. [CrossRef]
5. Huo, T.; Cao, R.; Du, H.; Zhang, J.; Cai, W.; Liu, B. Nonlinear influence of urbanization on China's urban residential building carbon emissions: New evidence from panel threshold model. *Sci. Total Environ.* **2021**, *772*, 145058. [CrossRef]
6. Liu, P.; Lin, B.; Zhou, H.; Wu, X.; Little, J. CO_2 emissions from urban buildings at the city scale: System dynamic projections and potential mitigation policies. *Appl. Energy* **2020**, *277*, 115546. [CrossRef]
7. Shareef, S. The impact of urban morphology and building's height diversity on energy consumption at urban scale. The case study of Dubai. *Build. Environ.* **2021**, *194*, 107675. [CrossRef]

8. Lau, S.; Yang, F.; Tai, J.; Wu, X.; Wang, J. The Study of Summer-time Heat Island, Built Form and Fabric in a Densely Built Urban Environment- Compact Chinese cities: Hong Kong, Guangzhou. *Int. J. Sustain. Dev.* **2011**, *14*, 30–48. [CrossRef]
9. Peng, L.; Jiang, Z.; Yang, X.; He, Y.; Xu, T.; Chen, S. Cooling effects of block-scale facade greening and their relationship with urban form. *Build. Environ.* **2020**, *169*, 106552. [CrossRef]
10. Shahrestani, M.; Yao, R.; Luo, Z.; Turkbeyler, E.; Davies, H. A field study of urban microclimates in London. *Renew. Energy* **2015**, *73*, 3–9. [CrossRef]
11. Sobstyl, J.M.; Emig, T.; Qomi, M.J.A.; Ulm, F.J.; Pellenq, J.M. Role of city texture in urban heat islands at nighttime. *Phys. Rev. Lett.* **2018**, *120*, 108701. [CrossRef]
12. Ye, H.; Hu, X.; Ren, Q.; Lin, T.; Li, X.; Zhang, G.; Shi, L. Effect of urban micro-climatic regulation ability on public building energy usage carbon emission. *Energy Build.* **2017**, *154*, 553–559. [CrossRef]
13. Ye, H.; Yan, H.; Hu, X.; Wang, D. Urban form optimization for low carbon building construction. In *Reference Module in Earth Systems and Environmental Sciences*; Elsevier: Amsterdam, The Netherlands, 2019.
14. Shi, Y.; Ren, C.; Zheng, Y.; Ng, E. Mapping the urban microclimatic spatial distribution in a sub-tropical high-density urban environment. *Archit. Sci. Rev.* **2015**, *59*, 370–384. [CrossRef]
15. Allen-Dumas, M.; Rose, A.; New, J.; Omitaomu, O.; Yuan, J.; Branstetter, M.; Sylvester, L.; Seals, M.; Carvalhaes, T.; Adams, M.; et al. Impacts of the morphology of new neighborhoods on microclimate and building energy. *Renew. Sustain. Energy Rev.* **2020**, *133*, 110030. [CrossRef]
16. Bat, A.; Romani, Z.; Bozonnet, E.; Draoui, A. Thermal impact of street canyon microclimate on building energy needs using TRNSYS: A case study of the city of tangier in morocco. *Case Stud. Therm. Eng.* **2021**, *24*, 100834. [CrossRef]
17. Cardinali, M.; Pisello, A.L.; Piselli, C.; Pigliautile, I.; Cotana, F. Microclimate mitigation for enhancing energy and environmental performance of near zero energy settlements in Italy. *Sustain. Cities Soc.* **2020**, *53*, 101964. [CrossRef]
18. Couch, C.; Dennemann, A. Urban regeneration and sustainable development in Britain. *Cities* **2000**, *17*, 137–147. [CrossRef]
19. Marker, B. Foundations of the sustainable compact city. *Glob. Built Environ. Rev.* **2005**, *4*, 19–23.
20. Angel, S.; Franco, S.; Liu, Y.; Blei, A. The shape compactness of urban footprints. *Prog. Plan.* **2020**, *139*, 100429. [CrossRef]
21. Kaza, N. Urban form and transportation energy consumption. *Energy Policy* **2020**, *136*, 111049. [CrossRef]
22. Lee, J.; Lim, S. The selection of compact city policy instruments and their effects on energy consumption and greenhouse gas emissions in the transportation sector: The case of south Korea. *Sustain. Cities Soc.* **2018**, *37*, 116–124. [CrossRef]
23. Matsuhashi, K.; Ariga, T. Estimation of passenger car CO_2 emissions with urban population density scenarios for low carbon transportation in japan. *IATSS Res.* **2016**, *39*, 117–120. [CrossRef]
24. Quan, S.; Li, C. Urban form and building energy use: A systematic review of measures, mechanisms, and methodologies. *Renew. Sustain. Energy Rev.* **2021**, *139*, 110662. [CrossRef]
25. Ewing, R.; Rong, F. The impact of urban form on U.S. residential energy use. *Hous. Policy Debate* **2008**, *19*, 1–30. [CrossRef]
26. Liu, X.; Sweeney, J. Modelling the impact of urban form on household energy demand and related co_2 emissions in the greater Dublin region. *Energy Policy* **2012**, *46*, 359–369. [CrossRef]
27. Trepci, E.; Maghelal, P.; Azar., E. Effect of densification and compactness on urban building energy consumption: Case of a Transit-Oriented Development in Dallas, TX. *Sustain. Cities Soc.* **2020**, *56*, 101987. [CrossRef]
28. Ye, H.; He, X.Y.; Song, Y.; Li, X.; Zhang, G.; Lin, T.; Xiao, L. A sustainable urban form: The challenges of compactness from the viewpoint of energy consumption and carbon emission. *Energy Build.* **2015**, *93*, 90–98. [CrossRef]
29. Ahmadian, E.; Sodagar, B.; Bingham, C.; Elnokaly, A.; Mills, G. Effect of urban built form and density on building energy performance in temperate climates. *Energy Build.* **2021**, *236*, 110762. [CrossRef]
30. Mangan, S.; Oral, G.; Kocagil, I.; Sozen, I. The impact of urban form on building energy and cost efficiency in temperate-humid zones. *J. Build. Eng.* **2020**, *33*, 101626. [CrossRef]
31. Oh, M.; Jang, K.M.; Kim, Y. Empirical analysis of building energy consumption and urban form in a large city: A case of Seoul, South Korea. *Energy Build.* **2021**, *245*, 111046. [CrossRef]
32. Ye, H.; Ren, Q.; Shi, L.; Song, J.; Hu, X.; Li, X.; Zhang, G.; Lin, T.; Xue, X. The role of climate, construction quality, microclimate, and socio-economic conditions on carbon emissions from office buildings in china. *J. Clean. Prod.* **2018**, *171 Pt 2*, 911–916. [CrossRef]
33. Ye, H.; Ren, Q.; Hu, X.; Lin, T.; Li, S.; Zhang, G.; Li, X. Modeling energy-related CO_2 emissions from office buildings using general regression neural network. *Resour. Conserv. Recycl.* **2018**, *129*, 168–174. [CrossRef]
34. Ye, H.; Qiu, Q.; Zhang, G.; Lin, T.; Li, X. Effects of natural environment on urban household energy usage carbon emissions. *Energy Build.* **2013**, *65*, 113–118. [CrossRef]
35. Zheng, S.; Wang, R.; Glaeser, E.L.; Kahn, M.E. The greenness of china: Household carbon dioxide emissions and urban development. *J. Econ. Geogr.* **2010**, *11*, 761–792. [CrossRef]
36. Hu, X. The Effects of Urban Compact Form on the Carbon Emissions from Residential Building Energy Consumption. Master's Thesis, University of Chinese Academy of Sciences, Beijing, China, 2017. (In Chinese).
37. Liu, Z.; Wang, S.; Liu, J.; Liu, F.; Fu, X. Analysis of factors affecting CO_2 emissions by civil buildings in china's urban areas. *Int. J. Energy Sci.* **2015**, *3*, 238–241. [CrossRef]
38. Peng, H.; Xue, Y.; Zhai, Z. Methods to Compare the Effects of Human Behavior Patterns in Different Climate Zones on Energy Consumption in Residential Buildings. *Build. Energy Environ.* **2020**, *225*, 4–10+15. (In Chinese)

39. Yang, X.; Zhao, L. Impacts of Urban Microclimate on Building Energy Performance: A Review of Research Methods. *Build. Sci.* **2015**, *31*, 1–7. (In Chinese) [CrossRef]
40. Mahesh, S.; Jayas, D.S.; Paliwal, J.; White, N.D.G. Comparison of partial least squares regression (PLSR) and principal components regression (PCR) methods for protein and hardness predictions using the near-infrared (NIR) hyperspectral images of bulk samples of Canadian wheat. *Food Bioprocess Technol.* **2015**, *8*, 31–40. [CrossRef]
41. Zhang, M.; Mu, H.; Li, G.; Ning, Y. Forecasting the transport energy demand based on PLSR method in China. *Energy* **2009**, *34*, 1396–1400. [CrossRef]
42. Thinh, N.X.; Arlt, G.; Heber, B.; Hennersdorf, J.; Lehmann, I. Evaluation of urban land-use structures with a view to sustainable development. *Environ. Impact Assess. Rev.* **2002**, *22*, 475–492. [CrossRef]
43. Zhao, J.; Song, Y.; Shi, L.; Tang, L. Study on the compactness assessment model of urban spatial form. *Acta Ecol. Sin.* **2011**, *21*, 37–42. (In Chinese)
44. Hu, X.; Yan, H.; Wang, D.; Zhao, Z.; Zhang, G.; Lin, T.; Ye, H. A Promotional Construction Approach for an Urban Three-Dimensional Compactness Model—Law-of-Gravitation-Based. *Sustainability* **2020**, *12*, 6777. [CrossRef]
45. Ye, H.; Hu, X.; Yan, H.; Zhang, G. A Kind of Standardized Urban Spatial Shape Compactedness Measurement Method and System. CN109977600A, 5 July 2019. (In Chinese).
46. Tan, X.; Deng, J. Grey relational analysis: A new method of multi factor statistical analysis. *Stat. Res.* **1995**, *12*, 46–48. (In Chinese)
47. Duan, H.; Chen, S.; Liu, Y.; Zhang, S.; Wang, X.; Wang, S.; Song, J. Characteristics of regional energy consumption of China's construction industry from the perspective of life cycle. *China Popul. Resour. Environ.* **2020**, *30*, 57–65. (In Chinese)
48. Li, H.; Qiu, P.; Wu, T. The regional disparity of per-capita CO_2 emissions in China's building sector: An analysis of macroeconomic drivers and policy implications. *Energy Build.* **2021**, *244*, 111011. [CrossRef]
49. Liu, X.; Hu, S.; Li, L. Temporal and spatial changes of building energy consumption in China's province and analysis of its influencing factors. *Math. Pract. Theory* **2020**, *50*, 76–87. (In Chinese)
50. Stevens, V.; Kotol, M.; Grunau, B.; Craven, C. The effect of thermal mass on annual heat load and thermal comfort in cold climate construction. *J. Cold Reg. Eng.* **2016**, *30*, 04015002. [CrossRef]
51. Du, K.; Yu, Y.; Wei, C. Climatic impact on china's residential electricity consumption: Does the income level matter? *China Econ. Rev.* **2020**, *63*, 101520. [CrossRef]
52. Namazkhan, M.; Albers, C.; Steg, L. A decision tree method for explaining household gas consumption: The role of building characteristics, socio-demographic variables, psychological factors and household behavior. *Renew. Sustain. Energy Rev.* **2019**, *119*, 109542. [CrossRef]
53. Zhou, S.; Teng, F. Estimation of urban residential electricity demand in china using household survey data. *Energy Policy* **2013**, *61*, 394–402. [CrossRef]
54. Tang, Y.; Song, Y.; Xie, J. Urban compactness changes in China from 2000 to 2010. *Ecol. Sci.* **2016**, *3*, 134–139. (In Chinese) [CrossRef]
55. Jia, Y.; Tang, L.; Gui, L. Study on the formulation and application of the urban spatial form dispersion index (NDIS). *Acta Ecol. Sin.* **2018**, *38*, 7269–7275. (In Chinese)
56. Wang, F.; Wen, A. A study of correlationship between the three-dimensional urban and urban thermal environment—A case study on JinPu district. *Territ. Nat. Resour. Study* **2016**, *4*, 70–72. (In Chinese)
57. Kondo, A.; Ueno, M.; Kaga, A.; Yamaguchi, K. The influence of urban canopy configuration on urban albedo. *Bound. Layer Meteorol.* **2001**, *100*, 225–242. [CrossRef]
58. Aida, M. Urban albedo as a function of the urban structure—A model experiment. *Bound. Layer Meteorol.* **1982**, *23*, 405–413. [CrossRef]
59. Grimmond, S.U.E. Urbanization and global environmental change: Local effects of urban warming. *Geogr. J.* **2007**, *173*, 83–88. [CrossRef]
60. Yang, X.; Li, Y. The impact of building density and building height heterogeneity on average urban albedo and street surface temperature. *Build. Environ.* **2015**, *90*, 146–156. [CrossRef]
61. Ignatius, M.; Hien, W.N.; Jusuf, S.K. Urban microclimate analysis with consideration of local ambient temperature, external heat gain, urban ventilation, and outdoor thermal comfort in the tropics. *Sustain. Cities Soc.* **2015**, *19*, 121–135. [CrossRef]
62. Yang, F.; Qian, F.; Lau, S.S.Y. Urban form and density as indicators for summertime outdoor ventilation potential: A case study on high-rise housing in Shanghai. *Build. Environ.* **2013**, *70*, 122–137. [CrossRef]
63. Peng, F.; Wong, M.; Ho, H.; Nichol, J.; Chan, P. Reconstruction of historical datasets for analyzing spatiotemporal influence of built environment on urban microclimates across a compact city. *Build. Environ.* **2017**, *123*, 649–660. [CrossRef]
64. Stromann-Andersen, J.; Sattrup, P.A. The urban canyon and building energy use: Urban density versus daylight and passive solar gains. *Energy Build.* **2011**, *43*, 2011–2020. [CrossRef]
65. Shang, C. Simulating the Impact of Urban Morphology on Energy Demand—A Case Study of Yuehai Eco-city, Yinchuan. *Archit. Cult.* **2018**, *12*, 166–168. (In Chinese) [CrossRef]
66. Zhou, W.; Huang, G.; Cadenasso, M.L. Does spatial configuration matter? Understanding the effects of land cover pattern on land surface temperature in urban landscapes. *Landsc. Urban Plan.* **2011**, *102*, 54–63. [CrossRef]
67. Haaland, C.; Bosch, C.K.V.D. Challenges and strategies for urban green-space planning in cities undergoing densification: A review. *Urban For. Urban Green.* **2015**, *14*, 760–771. [CrossRef]

68. Cheng, V.; Steemers, K.; Montavon, M.; Compagnon, R. Urban Form, Density and Solar Potential. In Proceedings of the PLEA2006—The 23rd Conference on Passive and Low Energy Architecture, Geneva, Switzerland, 6–8 September 2006.
69. Li, C.; Song, Y.; Kaza, N.; Burghardt, R. Explaining spatial variations in residential energy usage intensity in Chicago: The role of urban form and geomorphometry. *J. Plan. Educ. Res.* **2019**. [CrossRef]
70. Martins, T.; Adolphe, L.; Bonhomme, M. Building energy demand based on urban morphology analysis. *Appl. Mech. Mater.* **2007**, *10–12*, 737–741. [CrossRef]
71. Guo, G.; Wu, Z.; Chen, Y. Evaluation of spatially heterogeneous driving forces of the urban heat environment based on a regression tree model. *Sustain. Cities Soc.* **2020**, *54*, 101960. [CrossRef]
72. Jonghoon, P.; Jun-Hyun, K.; Bruce, D.; Kun, L.D. The role of green roofs on microclimate mitigation effect to local climates in summer. *Int. J. Environ. Res.* **2018**, *12*, 671–679. [CrossRef]
73. Sun, C.; Lin, T.; Zhao, Q.; Li, X.; Ye, H.; Zhang, G.; Liu, X.; Zhao, Y. Spatial pattern of urban green spaces in a long-term compact urbanization process—A case study in China. *Ecol. Indic.* **2017**, *96*, 111–119. [CrossRef]
74. Peng, J.; Jia, J.; Liu, Y.; Li, H.; Wu, J. Seasonal contrast of the dominant factors for spatial distribution of land surface temperature in urban areas. *Remote Sens. Environ.* **2018**, *215*, 255–267. [CrossRef]